



RESEARCH ARTICLE

10.1002/2017RS006335

Key Points:

- Estimation of the small-scale distribution parameters at the 94 GHz band in line-of-sight condition in the frequency domain
- Weibull is the best fit distribution using the Kolmogorov-Smirnov test
- The distribution alpha-mu provides the best fitting to the measurements for the lower tails of the distribution

Correspondence to:

J. Reig,
jreigp@dcom.upv.es

Citation:

Reig, J., M. T. Martinez-Ingles, J. M. Molina-Garcia-Pardo, L. Rubio, and V. M. Rodrigo-Peñarrocha (2017), Small-scale distributions in an indoor environment at 94 GHz, *Radio Sci.*, 52, 852–861, doi:10.1002/2017RS006335.


Received 11 APR 2017

Accepted 16 JUN 2017

Accepted article online 19 JUN 2017

Published online 15 JUL 2017

Small-scale distributions in an indoor environment at 94 GHz

J. Reig¹ , M. T. Martinez-Ingles², J. M. Molina-Garcia-Pardo³, L. Rubio¹, and V. M. Rodrigo-Peñarrocha¹

¹Electromagnetic Radiation Group (GRE), Institute of Telecommunications and Multimedia Applications, Universitat Politècnica de València, Valencia, Spain, ²University Center of Defense, San Javier Air Force Base, MDE-UPCT, Murcia, Spain, ³Departamento de Tecnologías de la Información y las Comunicaciones, Murcia, Spain

Abstract In this paper, an extensive multiple-input multiple-output measurement campaign in a lab environment has been conducted at the 94 GHz band. Using a vector network analyzer, updown converters, and omnidirectional antennas displaced in virtual arrays, we have obtained an estimation of the distribution parameters for the most usual distributions employed in the small-scale fading modeling, i.e., Rayleigh, Rice, Nakagami-*m* and α - μ , by using statistical inference techniques. Moreover, in this scenario the best fit distribution to the experimental data is the Weibull distribution, using the Kolmogorov-Smirnov test. However, the α - μ distribution provides the best fitting to the experimental results in terms of the lower tails of the distributions.

1. Introduction

The requirements of ultrabroadband besides the extremely high cellular capacity per square meter in 5G systems lead to explore new frequency bands beyond 6 GHz, in particular, the millimeter wave (mmW) bands [Rangan *et al.*, 2014]. Moreover, the requirement of massive multiple-input multiple-output (MIMO) in 5G, with large antenna arrays as many as 8 to 64 elements at transmitter (Tx) and receiver (Rx) sides, makes these bands attractive for the deploying of future 5G networks with high capacity.

According to Cudak *et al.* [2013], the range for the mmW bands is very limited, e.g., 11.3 m, 8.2 m, and 7.7 m for 60 GHz, 75 GHz, and 95 GHz, respectively, for downlink, line-of-sight (LOS) conditions, 10.8 Gbps, and a time division duplexing cycle of 50/50. Therefore, these mmW bands will probably be dedicated to indoor environments.

In spite of the fact that various studies in the literature on the W-band propagation (75–110 GHz) date from the 1990s [Kajiwara, 1995; Helminger *et al.*, 1998], recently, several efforts are being made to explore this band for indoor cellular systems [Thomas *et al.*, 2015; Maccartney *et al.*, 2015]. In particular, measurements at 94 GHz were carried out in Kajiwara [1995] and Helminger *et al.* [1998] mainly focused on characterizing the propagation losses and shadowing in indoor environments. Nevertheless, several small-scale fading analyses [Thomas *et al.*, 1994; Moon-Soon *et al.*, 2005; Reig *et al.*, 2014] have been carried out at the 60 GHz band, so far. In Thomas *et al.* [1994], values of the Rician *K*-factor have been reported in measurements performed in corridors of an office block in LOS condition modeled as a Rice distribution using an open-ended waveguide (OWG) and lens as antennas. In this work the values of the Rician *K*-factor ranged from 2.9 to 5.2 dB and from 0.6 to 1.5 dB using OWG and lens, respectively. In Moon-Soon *et al.* [2005], the Rayleigh distribution turned out to be the best fit distribution in urban environments with ranges up to 400 m. An extensive analysis of the small-scale fading amplitude has been conducted in Reig *et al.* [2014] by comparing the Rayleigh, Nakagami-*m*, Weibull, Rice, and α - μ distributions with the experimental distribution in a lab with LOS condition. In this work, the small-scale amplitude has been found to be best fitted by a Rice distribution, with Rician *K*-factors which ranges from 3.21 to 8.45 dB.

Nevertheless, to the best of the authors' knowledge, no further analysis of the small-scale fading at 94 GHz has been performed yet.

In this work, from MIMO measurements in an indoor lab scenario, an extensive analysis of the small-scale distributions has been carried out at the 92.5–95.5 GHz band with LOS condition. The amplitude distribution has been modeled as Rayleigh, Rice, Weibull, Nakagami-*m*, and α - μ distributions. The results show that the best fit distribution is the Weibull distribution in contrast to the Rice distribution obtained at the 60 GHz band [Reig *et al.*, 2014].

This paper is organized as follows: first of all, the configuration and the main parameters of the measurements have been described in section 2. Second, the probability density functions (PDF) and the cumulative density functions (CDF) of the most employed distributions to model the small-scale amplitude are presented in section 3. Next, in section 4 the calculation of the matching of the lower tails of the analytical distributions to the experimental distribution is explained in detail. Section 5 includes the results of the Kolmogorov-Smirnov test, the parameters of the distributions, and the matching of the lower tail of the distributions. Finally, the conclusions are discussed in section 6.

2. Measurements Description

The scenario where the measurements were collected is a lab of the Cartagena University. The dimensions of the lab are $8 \times 4.8 \times 3.5$ m, and closets, desktops, chairs, and shelves can be found as furniture. One position was selected for the receiver, while 11 positions randomly distributed in the room were selected for the transmitter. Figure 1 shows a picture of the lab with the Tx and Rx antennas and positioners, and Figure 2 illustrates a map of the lab.

The channel sounder is based on a R&S ZVA 67 vector network analyzer (VNA) and updown converters [Martinez-Ingles *et al.*, 2016]. MIMO measurements were carried out with uniform rectangular array (URA) at Tx and uniform linear array (ULA) at Rx virtual systems. A 3 GHz span around 94 GHz was selected with 1024 frequency points and a bandwidth (BW) of 10 Hz for the intermediate frequency filter. The maximum filter BW is constrained by the antenna specifications. A BW of 10 Hz leads to a dynamic range of 107 dB without including the antennas.

Two identical omnidirectional antennas with linear polarization manufactured by Mi-Wave (WR-10) were selected. These antennas operating at 94 GHz have the following relevant parameters: BW 3 GHz, gain 2 dBi, typical nominal VSWR 1.5:1, beam width in elevation 30° , and omnidirectional in the E plane. In Figure 3, the radiation pattern of the Tx and Rx antennas in the E plane is plotted at the frequency of 94 GHz.

Measurements with a combination of two polarizations were collected, either horizontal Tx and horizontal Rx (HH) or vertical Tx and vertical Rx (VV). The Tx and Rx antennas were operated with Arrick Robotics positioners. For the URA Tx, measurements were performed over a 6×6 grid along the X and Y axes, and for the ULA Rx, five elements were equally spaced along the Y axis. To analyze the influence of both the spacing and the number of positions of the URA, two additional measurements were carried out with a 25×25 rectangular grid using URA in positions 8 and 12 with HH and VV polarizations, respectively. The separation in the grid for both ULA Tx and URA Rx was of 1 mm (0.31λ at 94 GHz), except for the position 8 with HH polarization where a grid separation of 0.89 mm (0.28λ at 94 GHz) was configured.

The measurements were carried out in stationarity conditions. During the measurements the lab was closed to keep the temperature in the room stable and to avoid phase variations in the measurement of the S_{21} scattering parameter. Table 1 shows the exact location of each position of the Tx, the Rx position, and the Tx-Rx separation distance. The height of the Tx and Rx antennas was 0.784 and 0.886 m, respectively.

3. Small-Scale Fading Distributions

In this section, both the PDFs and CDFs of the most employed distributions used to model the small-scale fading are described, i.e., Rayleigh, Rice, Weibull, Nakagami- m , and α - μ .

Note that the parameters of above distributions have been calculated by statistical inference using the estimators described in Reig *et al.* [2014] without any type of mathematical approximation of those PDFs and CDFs to the experimental PDF and CDF, respectively.

Using the VNA, the S_{21} scattering parameter has been measured to obtain a relative measurement of the received electric field strength. There is no need in calculating the absolute value of the electric field strength providing that this paper analyzes the amplitude variation not the absolute value. For the sake of simplicity, we will use the electric field strength instead of S_{21} data proportional to the electric field strength.

If r is the electric field strength in linear units, the electric field strength in logarithmic units is given by $R = 20 \log r = B \ln r$, where $B = 20/\ln 10$.



Figure 1. Lab with Tx and Rx antennas and positioners.

3.1. Rayleigh Distribution

If r follows a Rayleigh distribution, the PDF of R is given by

$$p_R(R) = \frac{1}{B\sigma^2} \exp\left(\frac{2R}{B} - \frac{\exp(2R/B)}{2\sigma^2}\right), \quad -\infty < R < \infty, \quad (1)$$

and the CDF of R is expressed as

$$F_R(R) = 1 - \exp\left(-\frac{\exp(2R/B)}{2\sigma^2}\right), \quad -\infty < R < \infty, \quad (2)$$

where $\sigma = \sqrt{E[R^2]}/2$, and $E[\cdot]$ denotes the expectation value.

3.2. Rice Distribution

The PDF and CDF of the Rice distribution expressed in logarithmic units can be written as

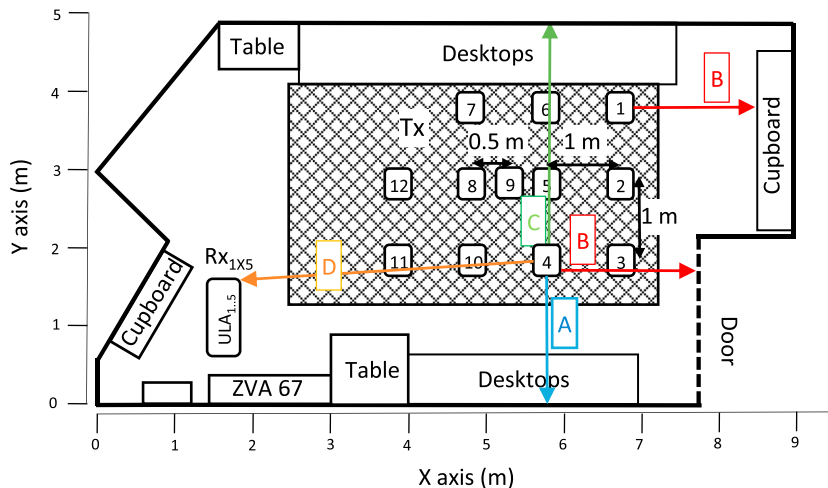


Figure 2. Map of the lab with distances of reference.

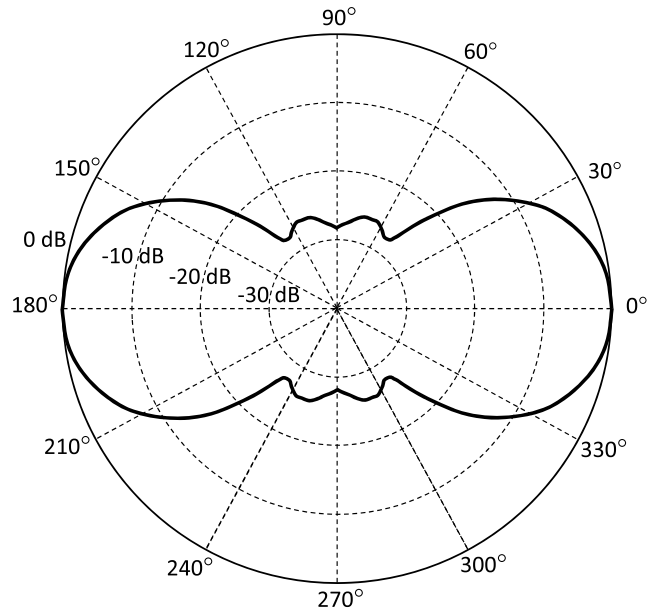


Figure 3. Radiation pattern in the E plane of the Tx and Rx antennas at 94 GHz.

$$p_R(R) = \frac{1}{B\sigma^2} \exp\left(\frac{2R}{B} - \frac{\exp(2R/B) + v^2}{2\sigma^2}\right) I_0\left(\frac{v \exp(R/B)}{\sigma^2}\right), \quad -\infty < R < \infty, \quad (3)$$

$$F_R(R) = 1 - Q_1\left(\frac{v}{\sigma}, \frac{\exp(2R/B)}{\sigma}\right), \quad -\infty < R < \infty, \quad (4)$$

where v^2 is the power of the dominant component, $2\sigma^2$ is the multipath power of the reflected and scattered components, $I_a(\cdot)$ is the modified Bessel function of the first kind with order a (formula 8.406 of *Gradshteyn and Ryzhik* [2007]), and $Q_1(a, b) = \int_b^\infty x \exp(-(x^2 + a^2)/2) I_0(ax) dx$ is the first-order Marcum Q -function [Marcum, 1950]. The Rician factor, denoted by K , extensively used in radio propagation is defined as

$$K = \frac{v^2}{2\sigma^2}, \quad (5)$$

which represents the ratio between the power of the coherent dominant component and the power of the reflected and scattered multipath contributions.

Table 1. Location of Tx and Rx and Tx and Rx Separation

Position Number	A (m)	B (m)	C (m)	Tx-Rx Separation D (m)
1	3.835	1.423	1.009	5.491
2	2.831	1.431	2.015	5.147
3	1.828	1.077	3.026	4.923
4	1.798	2.056	3.008	3.923
5	2.797	2.809	2.024	4.095
6	3.787	2.835	1.059	4.386
7	3.794	3.825	1.030	3.682
8	2.742	3.828	2.092	3.143
9	2.765	3.325	2.059	3.586
10	1.796	3.088	3.015	2.895
11	1.874	4.045	2.947	1.955
12	2.788	4.814	2.037	2.258
Rx ULA	1.620	5.985	3.220	

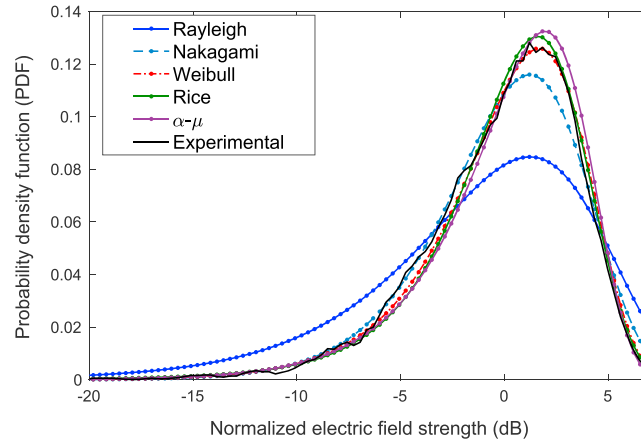


Figure 4. PDF of the normalized electric field strength for the Rayleigh, Nakagami- m , Weibull, Rice, α - μ , and experimental distributions in logarithmic units in the position 12 at the frequency of 92.5 GHz with VV polarization.

3.3. Nakagami- m Distribution

The PDF and the CDF of the Nakagami- m distribution in logarithmic units are given by

$$p_R(R) = \frac{2}{B\Gamma(m)} \left(\frac{m}{\Omega}\right)^m \exp\left(\frac{2mR}{B} - \frac{m \exp(2R/B)}{\Omega}\right), \quad -\infty < R < \infty, \quad (6)$$

$$F_R(R) = \gamma\left(m, \frac{m}{\Omega} \exp\left(\frac{2R}{B}\right)\right) / \Gamma(m), \quad -\infty < R < \infty, \quad (7)$$

where $\Gamma(\cdot)$ is the gamma function (formula 8.310 of *Gradshteyn and Ryzhik* [2007]); $\Omega = E[R^2]$ is the mean power; $m = \Omega^2 / \text{var}(R^2)$ is the fading parameter which provides information about the severity of fading, being $\text{var}(\cdot)$ the variance operator; and $\gamma(a, b) = \int_0^b t^{a-1} \exp(-t) dt$ is the lower incomplete gamma function (formula 8.350 of *Gradshteyn and Ryzhik* [2007]).

3.4. Weibull Distribution

The PDF and the CDF of the Weibull distribution in logarithmic units can be written as

$$p_R(R) = \frac{1}{B} \frac{\alpha R^{\alpha-1}}{\Omega^\alpha} \exp\left(\frac{\alpha}{B} R - \frac{1}{\Omega^\alpha} \exp\left(\frac{\alpha R}{B}\right)\right), \quad -\infty < R < \infty, \quad (8)$$

$$F_R(R) = 1 - \exp\left(-\frac{\exp(\alpha R/B)}{\Omega^\alpha}\right), \quad -\infty < R < \infty, \quad (9)$$

where α and $\Omega = \sqrt[\alpha]{E[R^\alpha]}$ are the shape and scale parameters of the Weibull distribution, respectively.

3.5. α - μ Distribution

The PDF and the CDF of the α - μ distribution in logarithmic units are given by

$$p_R(R) = \frac{1}{B} \frac{\alpha \mu^\mu R^{\alpha\mu-1}}{\Omega^{\alpha\mu} \Gamma(\mu)} \exp\left(\frac{\alpha \mu}{B} R - \frac{\mu}{\Omega^\alpha} \exp\left(\frac{\alpha R}{B}\right)\right), \quad -\infty < R < \infty, \quad (10)$$

$$F_R(R) = \gamma\left(\mu, \frac{\mu}{\Omega^\alpha} \exp\left(\frac{\alpha R}{B}\right)\right) / \Gamma(\mu), \quad -\infty < R < \infty, \quad (11)$$

where α is a parameter which controls the linearity, $\mu = E^2[R^\alpha] / \text{var}(R^\alpha)$ and $\Omega = \sqrt[\alpha]{E[R^\alpha]}$.

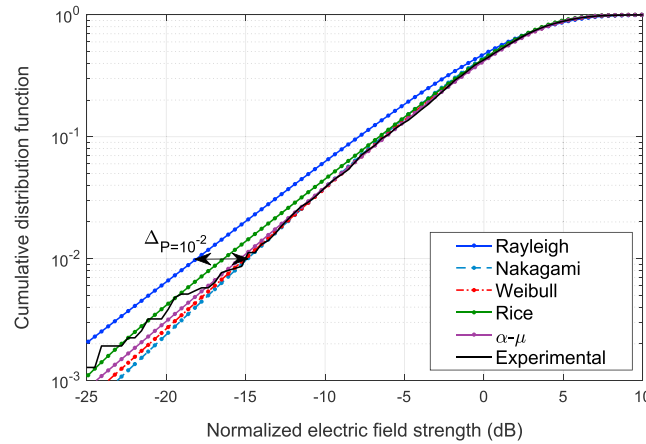


Figure 5. CDF of the normalized electric field strength for the Rayleigh, Nakagami- m , Weibull, Rice, α - μ , and experimental distributions in logarithmic units in the position 8 at the frequency of 92.7375 GHz with HH polarization.

we need to assess the behavior of the distribution specifically in the lower tails by using a procedure which evaluates the mismatch between the estimated and the experimental CDFs [Reig et al., 2014].

Let Δ_p be the difference between the electric field strength in logarithmic units of the estimated CDF and the electric field strength in logarithmic units of the experimental CDF for the same value of the CDF, P , defined as

$$\Delta_p = R_{est}^p - R_{exp}^p, \quad (12)$$

where R_{est}^p and R_{exp}^p are the values of the electric field strength in logarithmic units which satisfy $F_{est}(R_{est}^p) = P$ and $F_{exp}(R_{exp}^p) = P$, respectively; being $F_{est}(\cdot)$ the CDF of the estimated distribution, and $F_{exp}(\cdot)$ the CDF of the experimental distribution.

Figure 5 shows the CDF of the estimated distributions in logarithmic units given by (2), (4), (7), (9), and (11) together with the experimental CDF of the normalized electric field strength in logarithmic units for the position 8 with HH polarization at the frequency of 92.7375 GHz. In Figure 5, the difference $\Delta_{p=10^{-2}}$ has been illustrated for the Rayleigh distribution.

5. Results

In this section the results of the K-S test, the best fit distribution, the fading distribution parameters, and the statistical values of the difference in the lower tails of the distributions are analyzed.

In order to estimate the parameters of the distributions, 1024 distributions have been estimated in each one of the 11 positions with HH polarization and in each one of the 12 positions with VV polarization. Therefore, the total number of distributions to be estimated is $(11 + 12) \times 1024 = 23,552$. Each distribution consists of $n = 5 \times 6 \times 6 = 180$ samples, except for the positions 8 with HH polarization and 12 with VV polarization with $n = 5 \times 25 \times 25 = 3,125$ samples.

5.1. K-S Test and Best Fit Distribution

From the parameters estimated, we have evaluated the inferred Rayleigh, Rice, Nakagami- m , Weibull, and α - μ distributions for each frequency bin in each measurement. These distributions are compared to the experimental distributions by using the K-S test. The K-S test in one given frequency bin is fulfilled if the maximum absolute value between the experimental and the estimated CDFs, D_{est} , is lower or equal than a given value, $k_n(p)$, which depends on both the number of samples, n , and the significance level, p . Therefore, the condition to be accomplished in each frequency bin is as follows:

$$D_{est} = \max_{-\infty < R_j < \infty} (|F_{exp}(R_j) - F_{est}(R_j)|) \leq k_n(p), \quad (13)$$

where $k_n(p) = A/\sqrt{n}$, being $A = 1.36$ and 1.63 for $p = 5\%$ and 1% , respectively.

In Figure 4, the PDF of above distributions in logarithmic units given by (1), (3), (6), (8) and (10) is plotted beside the experimental distribution of the normalized electric field strength in logarithmic units for the position 12 at the frequency of 92.5 GHz with VV polarization.

4. Lower Tail of the Distributions

The fitting of the estimated to the experimental distributions in the lower tails affects significantly the wireless performance parameters, such as the bit error rate (BER) and the outage probability. Therefore, in addition to the Kolmogorov-Smirnov (K-S) test

Table 2. Best Fit Distributions Percentages and Kolmogorov-Smirnov Test Accomplishment Percentage for a Confidence Interval of 5%

	Polarization	Rayleigh	Nakagami- <i>m</i>	Weibull	Rice	α - μ
Best fit	HH	6.5	8.4	38	17.7	29.3
	VV	3.5	8.2	37.8	22.6	27.9
K-S 5%	HH	58.9	87.7	97.2	90.7	88.1
	VV	43.3	86.4	95.7	92.3	84.1

Table 2 shows the percentage of the fulfillment of the K-S test for a significance level of $p = 5\%$ and the percentage of the best fit for the above distributions over all the frequency bins of all the positions in each polarization combination, HH and VV. Each result of Table 2 with HH polarization corresponds to 11,264 distributions (11 positions \times 1024 bins of frequency). Also, 12,288 distributions (12 positions \times 1024 bins of frequency) have been analyzed for VV polarization.

The percentage of the best fit distribution has been calculated as the percentage of occurrence of the maximum value of D_{est} among the analyzed distributions. Note that the sum of the best fit percentages for each polarization combination is 100%.

We have highlighted both the maximum percentage of the best fit distribution occurrence and the maximum percentage of the K-S test accomplishment in bold letters.

The fulfillment percentage of the K-S test for a significance of 5% is considerably high, exceeding 84% for all the distributions except for the Rayleigh. The maximum value of accomplishment of the K-S test occurs in the Weibull distribution for both HH and VV polarizations. Also, the Weibull is the best fit distribution with a superior value of 38% and 37.8% with regard to the rest of distributions for HH and VV polarizations, respectively. In spite of LOS conditions, the Weibull is the best fit distribution to the measurement data.

5.2. Fading Distribution Parameters

Since the K-S test shows that the best distributions are the Weibull and Rice, an analysis of the parameters of such distributions has been carried out in this subsection.

Figure 6 shows the mean of the Rician K -factor in decibel, defined in (5), as a function of the frequency for the position 12 with VV polarizations. In this case, the variation of the mean of the Rician K -factor is substantial, decreasing from approximately 4 dB at 92.5 GHz to 0.5 dB at 94.5 GHz and growing from 0.5 dB at 94.5 GHz to 4.2 dB at 95.5 GHz.

In Figure 7, the mean of the Rician K -factor in dB is plotted as a function of the Tx and Rx separation distance for the HH and VV polarizations. Generally speaking, the mean values of the K parameter are small ranging from -2.05 to 4.72 dB and from -1.54 to 5.26 dB for the HH and VV polarizations, respectively. Also, the mean of the K parameter tends to decrease as the Tx and Rx separation increases. To illustrate this effect, solid lines

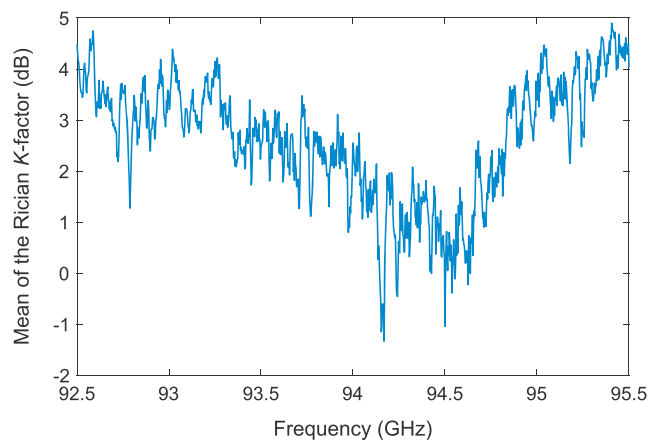


Figure 6. Mean of the Rician K -factor in dB as a function of the frequency for the position 12 and the polarization combination VV.

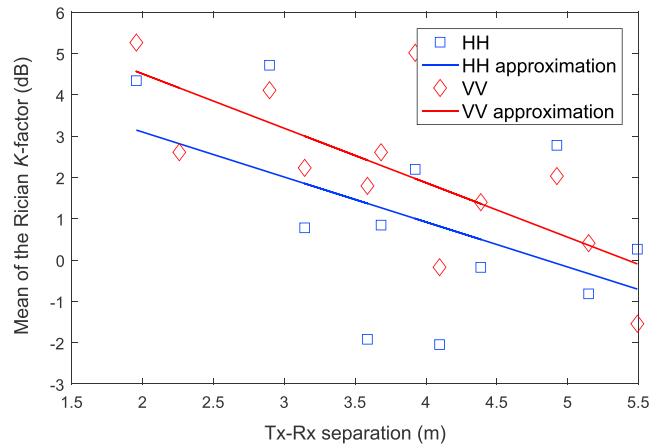


Figure 7. Mean of the Rician K -factor in dB as a function of Tx-Rx separation for HH and VV polarizations.

with the mean square error (MSE) approximation have been depicted for both polarizations. The mean of the K parameter in decibel can be approximated as a function of the Tx and Rx separation distance, d_{Tx-Rx} , expressed in m, for both polarization combinations as

$$\bar{K}_{HH} = -1.09d_{Tx-Rx} + 5.27 \quad \bar{K}_{VV} = -1.32d_{Tx-Rx} + 7.14. \quad (14)$$

Figure 8 shows the mean of the shape parameter, α , of the Weibull distribution. Note that the Weibull distribution turns into the Rayleigh distribution for $\alpha = 2$. The variation of the mean of α is significantly small, ranging from 2.08 to 3.29 and 2.1 to 3.29 with HH and VV polarizations, respectively. Again, mean values of α decrease as the Tx and Rx separation increases in a more noticeable way for the VV polarization, with the MSE approximations given by

$$\bar{\alpha}_{HH} = \begin{cases} -0.23d_{Tx-Rx} + 3.4 & d_{Tx-Rx} \leq 5.98 \text{ m} \\ 2 & d_{Tx-Rx} > 5.98 \text{ m} \end{cases} \quad (15)$$

$$\bar{\alpha}_{VV} = \begin{cases} -0.22d_{Tx-Rx} + 3.45 & d_{Tx-Rx} \leq 6.56 \text{ m} \\ 2 & d_{Tx-Rx} > 6.56 \text{ m} \end{cases} \quad (16)$$

Note that mean values of α lower than 2 correspond physically to composite small-scale and shadowing distributions, provided that in this case the Weibull distribution models worse scenarios than the Rayleigh

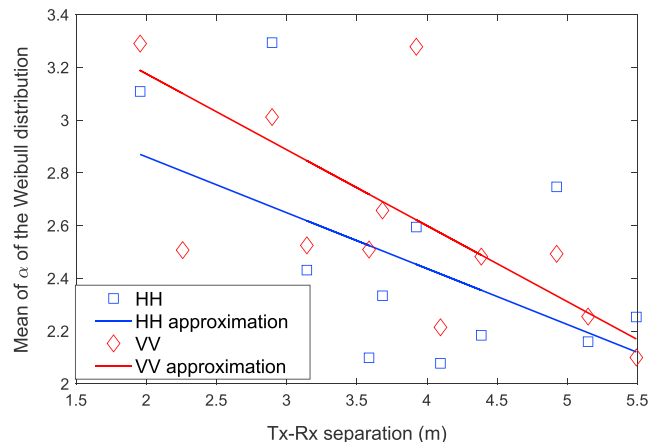


Figure 8. Mean of the α parameter of the Weibull distribution as a function of the Tx-Rx separation for HH and VV polarizations.

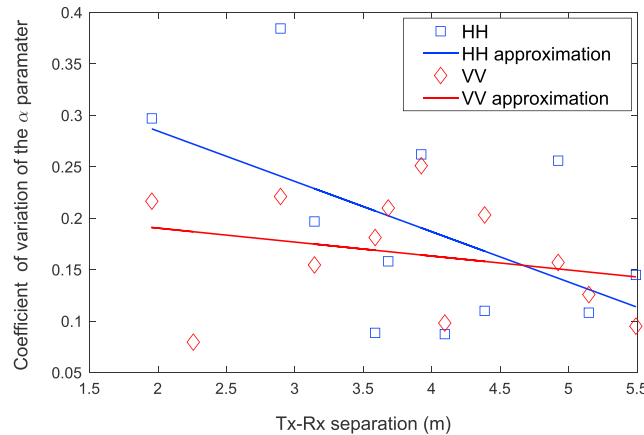


Figure 9. Coefficient of variation of the α parameter of the Weibull distribution as a function of Tx-Rx separation for HH and VV polarizations.

distribution. That fact can be explained by the following: the standard deviation of the received field strength in logarithmic units is given by $\sigma_R = (20/(\alpha \ln 10)) \sqrt{\psi'(1)}$, where $\psi'(\cdot)$ is the polygamma function of first order (formula 6.4.1 of Abramowitz [1972]). Therefore, the standard deviation of the received field strength decreases as α grows. Furthermore, the estimated Weibull distribution is equivalent to a Rayleigh distribution for $\alpha = 2$, and therefore, $\sigma_R = (10/(\ln 10)) \sqrt{\psi'(1)} = 5.57$ dB. Since the Rayleigh distribution describes the worst-case scenario corresponding to the small-

scale fading amplitude [Molisch, 2011], the fading amplitude distribution of the received field strength necessarily includes a long-term fading or shadowing variation for $\alpha < 2$.

Therefore, the estimated Weibull distribution is equivalent to a Rayleigh distribution ($\alpha = 2$) for Tx and Rx separations higher than 5.98 and 6.56 m for HH and VV polarizations, respectively.

In order to evaluate the dispersion of the estimated α values of the Weibull distribution, we have calculated the coefficient of variation of α defined as the ratio of the sample standard deviation to the sample mean of a distribution [Everitt and Skrondal, 2010].

Figure 9 shows the coefficient of variation for the estimated α parameter in the Weibull distribution in terms of the Tx-Rx separation for the HH and VV polarizations. Note that this coefficient of variation of the estimated α parameter for the Weibull distribution is the lowest of the coefficients of variation for the other parameters in the rest of distributions analyzed, i.e., Rayleigh, Rice, Nakagami- m , and α - μ . This coefficient of variation of the estimated Weibull α parameter remains under 0.3, and it tends to decrease with the Tx-Rx separation. Therefore, the trend to become a Rayleigh distribution is clear for high separations ($d_{Tx-Rx} \geq 5.5$ m), provided that α tends to 2 and the coefficient of variation of α is considerably small.

5.3. Lower Tail of the Distributions

Table 3 shows the mean and the root-mean-square (RMS) values for $\Delta_{P=10^{-1}}$ and $\Delta_{P=10^{-2}}$ of the estimated Rayleigh, Nakagami- m , Weibull, Rice, and α - μ distributions for the position 8 with HH polarization and the position 12 with VV polarization. Also, the mean and RMS values of $\Delta_{P=10^{-1}}$ have been calculated for the whole measurements in all the positions that comprise 23,552 distributions. The distributions with the smallest mean and RMS values are highlighted in bold letters. The values of $\Delta_{P=10^{-1}}$ and $\Delta_{P=10^{-2}}$ are low biased (small

Table 3. Mean and Root-Mean-Square (RMS) Values of the Difference Between the Normalized Electric Field Strength of the Estimated CDFs and the Normalized Electric Field Strength of the Experimental CDF in Logarithmic Units for the Same Value of the CDF, $P = 10^{-1}$ and $P = 10^{-2}$

	Position	P	Rayleigh	Nakagami- m	Weibull	Rice	α - μ
Mean (dB)	8HH	10^{-1}	-1.83	-0.26	-0.11	-0.18	0.01
		10^{-2}	-2.8	0.61	0.46	-0.11	0.05
	12VV	10^{-1}	-2.51	-0.44	-0.23	-0.17	-0.008
		10^{-2}	-3.40	1.11	0.89	-0.0006	0.21
RMS (dB)	All the positions	10^{-1}	-1.95	-0.19	-0.03	0.18	0.10
		10^{-2}	2.44	0.39	0.27	0.31	0.27
	8HH	10^{-1}	4.06	0.90	0.78	0.74	0.53
		10^{-2}	2.63	0.51	0.34	0.31	0.30
	12VV	10^{-1}	3.72	1.26	1.07	0.81	0.59
		10^{-2}	2.69	0.71	0.65	0.72	0.60

absolute values of the mean) except for the Rayleigh distribution. Also, the α - μ distribution provides the lowest RMS value of $\Delta_{p=10^{-1}}$ and $\Delta_{p=10^{-2}}$ (except for $\Delta_{p=10^{-2}}$ in the measurement 8 with HH polarization).

6. Conclusions

In this paper, the most commonly employed small-scale distributions to model the small-scale fading amplitude have been estimated from MIMO measurements conducted in a lab at the 94 GHz band with LOS condition for HH and VV polarization combinations. The results show that, in general, the Weibull distribution matches the best to the measurement records with a 92.7% and 95.7% of fulfillment of the K-S test with significance of 5% for HH and VV polarizations, respectively. The second best fit distribution is the Rice distribution with also high accomplishment of the K-S test (90.7% and 92.3% for HH and VV polarizations, respectively, with a significance of 5%). Low mean Rician K -factors have been estimated, smaller than approximately 0 dB for Tx and Rx separation distances higher than 5 m.

In terms of the tails of the distribution, the best distribution is the α - μ distribution. Moreover, in this environment the Weibull distribution tends to a Rayleigh distribution for Tx and Rx separations higher than approximately 6 m and 6.5 m with HH and VV polarizations, respectively.

Acknowledgments

This work was supported by the Ministerio de Economía y Competitividad MINECO, Spain (TEC2016-78028-C3-2-P) and by the European FEDER funds. Further information regarding the data obtained and included in this paper can be attained by contacting the author, Jose M. Molina (josemaria.molina@upct.es).

References

- Abramowitz, M. (1972), *Handbook of Mathematical Functions, With Formulas, Graphs, and Mathematical Tables*, 9th ed., Dover Publ.
- Cudak, M., A. Ghosh, T. Kovarik, R. Ratasuk, T. A. Thomas, F. W. Vook, and P. Moorut (2013), Moving towards Mmwave-based beyond-4G (B-4G) technology, in *Proc. VTC Spring—IEEE Vehicular Technology Conference Spring*, pp. 1–5, IEEE, doi:10.1109/VTCSpring.2013.6692638.
- Everitt B. S., and A. Skondal (2010), *The Cambridge Dictionary of Statistics*, 4th ed., Cambridge Univ. Press, Cambridge, U. K.
- Gradshteyn, I. S., and I. M. Ryzhik (2007), *Table of Integrals, Series and Products*, 7th ed., pp. 89–89, Academic Press, New York.
- Helminger J., J. Detlefsen, and H. Groll (1998), Propagation properties of an indoor-channel at 94 GHz, in *Proc. ICMMT International Conference on Microwave and Millimeter Wave Technology*, pp. 9–14, IEEE, Beijing, doi:10.1109/ICMMT.1998.768215.
- Moon-Soon, C., G. Grosskopf, and D. Rohde (2005), Statistical characteristics of 60 GHz wideband indoor propagation channel, in *Proc. 16th International Symposium on Personal, Indoor and Mobile Radio Communications-PIMRC*, vol. 1, pp. 599–603, IEEE, doi:10.1109/PIMRC.2005.1651506.
- Kajiwara A. (1995), Indoor propagation measurements at 94 GHz, in *Proc. 6th International Symposium on Personal, Indoor and Mobile Radio Communications-PIMRC*, vol. 3, pp. 1026–1030, IEEE, doi:10.1109/PIMRC.1995.477099.
- Maccartney G. R., T. S. Rappaport, S. Sun, and S. Deng (2015), Indoor office wideband millimeter-wave propagation measurements and channel models at 28 and 73 GHz for ultra-dense 5G wireless networks, *IEEE Access*, 3, 2388–2424, doi:10.1109/ACCESS.2015.2486778
- Marcum J. I. (1950), Table of Q functions, U.S. Air Force RAND Research Memorandum M-339. Santa Monica, Rand Corporation.
- Martinez-Ingles M. T., D. P. Gaillot, J. Pascual-Garcia, J. M. Molina-Garcia-Pardo, J. V. Rodriguez, L. Rubio, and L. Juan-Llacer (2016), Channel sounding and indoor radio channel characteristics in the W-band, in *Proc. EURASIP-Journal on Wireless Communications and Networking*, vol. 30, pp. 1–8, Springer, New York, doi:10.1186/s13638-016-0530-7.
- Molisch, A. F. (2011), *Wireless Communications*, 2nd ed., pp. 81–81, John Wiley, N. J.
- Rangan S., T. S. Rappaport, and E. Erkip (2014), Millimeter-wave cellular wireless networks: Potentials and challenges, *Proc. IEEE*, 102, 266–285, doi:10.1109/JPROC.2014.2299397
- Reig J., M. T. Martinez-Ingles, L. Rubio, V. M. Rodrigo-Peñarrocha, and J.-M. Molina-Garcia-Pardo (2014), Fading evaluation in the 60 GHz band in line-of-sight conditions, *Int. J. Antennas Propag.*, 1–12, doi:10.1155/2014/984102.
- Thomas H. J., R. S. Cole, and G. L. Siqueira (1994), An experimental study of the propagation of 55 GHz millimeter waves in an urban mobile radio environment, *IEEE Trans. Veh. Technol.*, 43, 140–146, doi:10.1109/25.282274.
- Thomas T. A., F. W. Vook, and S. Sun (2015), Investigation into the effects of polarization in the indoor mmWave environment, in *Proc. ICC-IEEE International Conference on Communications*, pp. 1386–1391, IEEE, U. K., doi:10.1109/ICC.2015.7248517.